Published in final edited form as:

Arch Biochem Biophys. 2008 May 1; 473(1): 69–75. doi:10.1016/j.abb.2008.02.033.

Cooperativity of cytochrome P450 1A2: Interactions of 1,4-phenylene diisocyanide and 1-isopropoxy-4-nitrobenzene

Emre M. Isin[1,2], **Christal D. Sohl**[1], **Robert L. Eoff**, and **F. Peter Guengerich**

Department of Biochemistry and Center in Molecular Toxicology, Vanderbilt University School of Medicine, Nashville, Tennessee 37232-0146

Abstract

Homotropic cooperativity of 1-alkoxy-4-nitrobenzene substrates and also their heterotropic cooperative binding interactions with the iron ligand 1,4-phenylene diisocyanide ($Ph(NC)_2$) had been demonstrated previously with rabbit cytochrome P450 (P450) 1A2 (Miller, G. P. and Guengerich, F. P. (2001) *Biochemistry 40*, 7262–7272). Multiphasic kinetics were observed for the binding of $Ph(NC)_2$ to both ferric and ferrous P450 1A2, including relatively slow steps. $Ph(NC)_2$ induced an apparently rapid change in the circular dichroism spectrum, consistent with a structural change, but had no effect on tryptophan fluorescence. $Ph(NC)_2$ binds the P450 iron in both the ferric and ferrous forms; ferric P450 1A2 was reduced rapidly in the absence of added ligands, and the rate was attenuated when $Ph(NC)_2$ was bound. No oxidation products of $Ph(NC)_2$ were detected. Docking studies with a rabbit P450 1A2 homology model based on the published structure of a human P450 1A2•α-naphthoflavone (αNF) complex indicated adequate room for a complex with either two 1-isopropoxy-4-nitrobenzene molecules or a combination of one 1-isopropoxy-4-nitrobenzene and one $Ph(NC)_2$; in the case of αNF no space for an extra ligand was available. The patterns of homotropic cooperativity seen with 1-alkoxy-4-nitrobenzenes (biphasic plots of v *vs.* S) differ from those seen with polycyclic hydrocarbons (positive cooperativity), suggesting that only with the latter does the ligand interaction produce improved catalysis. Consistent with this view, $Ph(NC)_2$ inhibited the oxidation of 1-isopropoxy-4-nitrobenzene and other substrates.

Address correspondence to: Prof. F. Peter Guengerich, Department of Biochemistry and Center in Molecular Toxicology, Vanderbilt University School of Medicine, 638 Robinson Research Building, 2200 Pierce Avenue, Nashville, Tennessee 37232-0146, Telephone: (615) 322-2261, FAX: (615) 322-3141, f.guengerich@vanderbilt.edu.

[1]These authors contributed equally and should be considered co-first authors.

[2]Current address: Biotransformation Section, Department of Discovery DMPK & Bioanalytical Chemistry, AstraZeneca R & D Mölndal, SE-431 83 Mölndal, Sweden.

Introduction

P450[3] enzymes play important roles in the metabolism of drugs, steroids, eicosanoids, fat-soluble vitamins, and carcinogens in mammals [2]. In the metabolism of drugs, ~75% of the reactions are catalyzed by P450s [3,4].

The P450s involved in drug metabolism have been studied extensively. One of the phenomena that is still not understood well is ligand cooperativity. Heterotropic cooperativity [5,6], in which one ligand stimulates catalysis involving another ligand (substrate), was first observed >35 years ago [7–9]. Homotropic cooperativity, recognized more recently [10,11], refers to several types of non-hyperbolic plots of v *vs.* S for a single substrate. A number of possible explanations have been proposed to explain cooperativity, including “classical” allosteric ligand site binding, multiplicity of ligand binding within a large active site, multiplicity of protein conformers, and protein subunit interactions [11–21].

Much of the research on P450 cooperativity has been directed towards several P450s now known to have large substrate binding sites, i.e. P450s 3A4, 2C8, and 2C9 [22–25]. P450 1A2 has a smaller active site, as revealed in the recently published crystal structure of a human P450 1A2•αNF complex [26]. Cooperativity has been described for rabbit P450 1A2 [27,28] and human P450 1A2 [28]. Homotropic cooperativity was seen in the *O*-dealkylation of 1-alkoxy-4-nitrobenzenes, with v *vs.* S plots being biphasic and characterized with two sets of k_{cat} and K_m values, with $K_{m,1} < K_{m,2}$ [27]. In that study, heterotropic cooperativity for ligand binding was observed in the interaction between 1-alkoxy-4-nitrobenzenes and an isocyanide, $Ph(NC)_2$.

Isocyanides have a long history in the study of hemoproteins, going back to work in 1929 with hemoglobin and methyl isocyanide [29]. Isocyanides were also used extensively in some of the early research on P450 [30–32]; the divalent carbon atom is liganded directly to either ferric or ferrous iron in the P450 [33] and yields a “Type II” Soret difference spectrum distinctly different than that often generated by the addition of substrates (low- to high-spin iron transition, “Type I”). Titrations of rabbit P450 1A2 with 1-alkoxy-4-nitrobenzenes and $Ph(NC)_2$ led to the conclusion that one ligand could enhance the binding of the other, indicative of multiple ligand occupancy as opposed to competition of the two ligands for a single site [27]. More recently, we have also observed homotropic cooperativity with P450 1A2 in pyrene 1-hydroxylation (and the subsequent hydroxylation(s) of 1-hydroxypyrene), with the v *vs.* S behavior fitting to highly sigmoidal plots with Hill coefficients (*n*) of 2 to 4 [28].

In the present work, several aspects of the interaction of $Ph(NC)_2$ with rabbit P4540 1A2 were studied, including kinetics of binding, conformational changes of the enzyme (as detected by CD spectroscopy), and effects on rates of P450 reduction and catalysis of P450 1A2 reactions. Modeling of the ligands was done using the published crystal structure of the human P450 1A2-αNF complex [26], which is now available as a template. The cooperative

[3]Abbreviations used: αNF, α-naphthoflavone (7,8-benzoflavone); $(CH_3)_2CH\text{-}OPhNO_2$, $(CH_3)_2CH\text{-}O\text{-}PhNO_2$; P450, cytochrome P450 (also termed “heme-thiolate protein P450 [1]; $Ph(NC)_2$, 1,4-phenylene diisocyanide.

interactions of the 1-alkoxy-4-nitrobenzenes and $Ph(NC)_2$ are rather different that those recently described for P450 1A2 and some polycyclic hydrocarbons [28].

Materials and methods

Chemicals

$Ph(NC)_2$ and αNF were purchased from Aldrich Chemical Co. (Milwaukee, WI). $Ph(NC)_2$ was recrystallized from hexanes. $(CH_3)_2CH$-O-$PhNO_2$ was synthesized as previously described [27] and recrystallized from a mixture of C_2H_5OH/H_2O.

Enzymes

P450 1A2 was purified from liver microsomes of rabbits treated with β-naphthoflavone using slight modification [34] of a previously described method [35]. Recombinant rat NADPH-P450 reductase was expressed in *Escherichia coli* and purified as described elsewhere [36].

Assays of product formation

Incubations included P450 1A2 (0.25 μM), NADPH-P450 reductase (0.50 μM), and L-α-dilauroyl-*sn*-glycero-3-phosphocholine (23 μM) in 0.10 M potassium phosphate buffer (pH 7.4) at 37 °C, using an NADPH-generating system [37], with either αNF (14 or 35 μM), $(CH_3)_2CH$-O-$PhNO_2$ (50 or 700 μM), or pyrene (35 or 140 μM). In the case of aniline, slight modifications in concentrations were made (3.3 μM P450 1A2, 6.6 μM NADPH-P450 reductase, 200 μM L-α-dilauroyl-*sn*-glycero-3-phosphocholine, and 8 mM aniline [30]). Incubations were done for 20 min in the case of the αNF, aniline, and $(CH_3)_2CH$-O-$PhNO_2$ experiments. αNF 5,6-epoxidation was analyzed by HPLC as described elsewhere [28,38]. $(CH_3)_2CH$-O-$PhNO_2$ *O*-dealkylation was monitored spectrophotometrically immediately after adding the NADPH-regenerating system (release of 4-nitrophenol, ΔA_{400}), as described previously, using the extinction coefficient of 4-nitrophenol, $\varepsilon_{400} = 12\ mM^{-1}\ cm^{-1}$ [27]. Rates of aniline 4-hydroxylation were estimated using a colorimetric procedure [39], utilizing an extinction coefficient for 4- aminophenol (generated with a standard curve), $\varepsilon_{630} = 10\ mM^{-1}\ cm^{-1}$ [40]. Pyrene 1- hydroxylation was analyzed by HPLC/fluorescence by slight modification of a procedure described elsewhere [28,41].

Spectroscopic measurements

Steady-state UV-visible spectroscopy was done using OLIS-Cary 14 and OLIS-Aminco DW2 instruments (On-Line Instrument Systems, Bogart, GA). Steady-state fluorescence measurements were made using an OLIS DM-45 instrument. Steady-state CD measurements were made with a JASCO 810 instrument (JASCO, Easton, MD) in the Vanderbilt Structural Biology facility. Stopped-flow UV-visible and fluorescence measurements were made using an OLIS RSM-1000 system (On-Line Instrument Systems) operating in the rapid-scanning mode. Stopped-flow CD measurements were made with a modified Applied Photophysics SX-17MV instrument (Applied Photophysics, Leatherhead, UK), kindly made available by R. N. Armstrong (Vanderbilt Univ.).

Anaerobic studies were done using custom-made glass cuvettes and tonometers and a vacuum/Ar manifold as described previously [42–44], including use of a glucose oxidase-catalase-glucose enzymatic scrubbing system and loading into the RSM-1000 stopped-flow spectrophotometer [44].

Homology model building

A crystal structure of a human P450 1A2-αNF complex [26] was used as the template to develop a homology model of rabbit P450 1A2 utilizing the automated homology modeling tool SWISS-MODEL [45]. Coordinate files for molecules of $(CH_3)_2CH$-O-$PhNO_2$ and $Ph(NC)_2$ were generated using the Dundee PRODRG2 server [46] and manually docked into the binding cavity (replacing αNF) using Turbo Frodo.[4] Simulated annealing was then performed with the program CNS Solve 1.1 using the input file model Anneal [47,48]. The heme group was fixed during simulated annealing (energy-minimized models were not adjusted following annealing).

Results

Kinetics of ligand binding to ferric P450 1A2

Binding of the Type II ligand $Ph(NC)_2$ to ferric P450 1A2 was slow (Fig. 1), with estimated rates of 0.07 and 0.01 s^{-1} using a bi-exponential fit, at a final ligand concentration of 100 μM. Binding of the substrate $(CH_3)_2CH$-O-$PhNO_2$ (data not presented) was also biphasic and relatively slow, with rates of 2.9 and 0.08 s^{-1} measured at a substrate concentration of 10 μM [28].

Kinetics of binding of $Ph(NC)_2$ to ferrous P450 1A2

The ferrous P450-$Ph(NC)_2$ complex had a strong absorption maximum at 455 nm, typical of isocyanide complexes [32,33], which can be used for kinetic analysis of binding. The binding of $Ph(NC)_2$ to ferrous P450 was triphasic, with a rapid burst followed by a biphasic change that accounted for most of the absorbance increase (Figs. 2a, 2b). When the rates were measured as a function of $Ph(NC)_2$ concentration, the fast phase yielded an apparent rate constant of 1.4×10^6 M^{-1} s^{-1} (Fig. 2c) but the rates of the latter two steps were rather invariant with the concentration (Fig. 2d).

CD and fluorescence spectra

The binding of either $(CH_3)_2CH$-O-$PhNO_2$ or $Ph(NC)_2$ to P450 1A2 induced changes in the CD spectrum (Fig. 3). The far-UV changes are indicative of a change in the conformation of the protein and consistent with a decrease (based on $[\theta_{220}]$) in α-helicity [49].

Changes in the Trp fluorescence of P450 1A2 have been observed upon binding of 1-alkoxy-4-acetanilides [50]. We also attempted to monitor the binding of $Ph(NC)_2$ to P450 1A2 using a decrease (or increase) in P450 Trp fluorescence, but no changes were observed (for Trp or Tyr).

[4]Cambillau, C., and Roussel, A. (1997) Turbo Frodo, Version OpenGL.1, Université Aix-Marseille II, Marseille, France.

Effect of $Ph(NC)_2$ on catalytic activity of P450 1A2

In the early literature on P450, diethylisocyanide was reported to stimulate the oxidation of aniline in rabbit liver microsomes [30,32]. The enhanced spectral changes in substrate binding with the presence of $Ph(NC)_2$ [27] raised the possibility of stimulation of P450 1A2 activity. However, $Ph(NC)_2$ inhibited $(CH_3)_2CH$-O-$PhNO_2$ *O*-dealkylation and aniline 4-hydroxylation (Fig. 4), as well as αNF 5,6-epoxidation and pyrene 1- hydroxylation (results not shown).

$Ph(NC)_2$ was not converted to any products detected using general HPLC-UV profiling by rabbit P450 1A2 (< 0.01 nmol of any product min^{-1} (nmol P450)$^{-1}$, assuming a similar extinction coefficient).

Effect of $Ph(NC)_2$ on rate of P450 1A2 reduction

One of the interesting features of isocyanides is that, in contrast to other Type II P450 ligands, they bind to both ferric and ferrous P450 heme and the complexes can be discerned spectrally (Fig. 5). We were able to examine the effect of $Ph(NC)_2$ on the rate of reduction of P450 1A2, which was a 10-fold attenuation (Fig. 5). However, even the attenuated rate (of heme reduction) is considerably faster than rates of substrate oxidation, and the inhibition of catalytic activity (Fig. 4) is not the result of only the decreased reduction rate. To our knowledge, a direct examination of the rates of electron transfer from NADPH-P450 reductase to a P450 with its heme iron liganded to a Type II ligand have not been determined previously, mainly because many ligands have similar spectra in the ferric and ferrous states (e.g., cyanide or azoles) and use of CO as a trap would require a dissociation step.

Fitting of ligands in a homology model of P450 1A2

The possibility of simultaneous binding of $(CH_3)_2CH$-O-$PhNO_2$ and $Ph(NC)_2$ in the active site of rabbit P450 1A2, hypothesized earlier [27], was examined by docking the ligands into the active site of a homology model based on a human P450 1A2-αNF complex [26] (Fig. 6a). As with pyrene [28], both molecules can easily fit into the active site of the model, regardless of which ligand is bound closest to the heme group (Fig. 6b, 6c). Except for the disruption of the F-helix, which was observed in the human P450 1A2-αNF structure [26], none of the α-helices that comprise the active-site pocket are disrupted by the simultaneous presence of $(CH_3)_2CH$-O-$PhNO_2$ and $Ph(NC)_2$.

Discussion

The previous conclusion that both a 1-alkoxy-4-ntrobenzene and $Ph(NC)_2$ could co-occupy the active site of P450 1A2 [27] is consistent with the protein model (Fig. 6). The model is considered reliable in that the rabbit P450 1A2 sequence has high identity (75%) with the human P450 1A2 sequence [52] and the two proteins have many similar functional characteristics [34]. The rabbit protein was used both in the previous [27] and the present studies because human P450 1A2 is isolated almost exclusively in the high-spin state [26,34] and the spectral studies with substrate binding cannot be done (at least using heme Soret perturbation approaches). The rabbit P450 1A2 used in this study was estimated to be

77% low-spin iron [28], as judged by second-derivative spectroscopy of the Soret band [53,54]. Although the protein used in these studies was isolated from rabbit liver microsomes, there was no evidence of another P450 or other impurity (i.e., sodium dodecyl sulfate polyacrylamide gel electrophoresis), and previous work with recombinant rabbit P450 1A2 showed the major cooperative features of the protein purified from liver [27].

The kinetics of binding of $Ph(NC)_2$ were different for ferric and ferrous P450 (Figs. 1, 2). Binding to ferrous P450 1A2 showed a fast phase (Fig. 2a), followed by what appear to be two much slower phases (Fig. 2b). The rate of the fast phase increased with tc), while the two slower steps were rather invariant with the concentration (Fig. 2d). With ferric P450 (Fig. 1), only a slow biphasic change was seen, and the rates are similar to those of the second two steps with the reduced enzyme (Figs. 2b, 2d). The concentration dependence of the rates of the two steps in Fig. 1 was not examined. The similarity of the rates of the two slow steps in the ferrous and ferric reactions is not due to oxidation of the ferrous to the ferric state because the absorbance wavelength used (455 nm) is only indicative of binding to the ferrous iron (Fig. 5b). Our conclusion is that the fast rate constant with the ferrous enzyme ($1.4 \times 10^6\ M^{-1}\ s^{-1}$) might represent the second-order “on” rate (although this is somewhat slow [55]) and the slower rates observed with both ferric and ferrous P450 represent conformational events in changing the protein to achieve the final spectrum. We emphasize that the multiphasic kinetics of ligand binding do not constitute any evidence for multiple ligand occupancy, in the absence of other data.

The homology model (Fig. 6) is considered reliable, at least for a ground state P450 1A2-substrate complex [26]. The active site (estimated size 375 $Å^3$ [26]) is large enough to fit only one αNF molecule [26] or two pyrenes [28] but either two molecules of $(CH_3)_2CH\text{-}O\text{-}PhNO_2$, two molecules of $Ph(NC)_2$, or one of each ($(CH_3)_2CH\text{-}O\text{-}PhNO_2$, $Ph(NC)_2$) (Fig. 6). We propose that the co-occupancy by two molecules of $(CH_3)_2CH\text{-}O\text{-}PhNO_2$ may be responsible for the two-k_{cat}, two-K_m behavior (“negative cooperativity”) observed for $(CH_3)_2CH\text{-}O\text{-}PhNO_2$ *O*-dealkylation [27]. Fitting of one molecule each of $(CH_3)_2CH\text{-}O\text{-}PhNO_2$ and $Ph(NC)_2$ into the model of the active site (Fig. 6) is consistent with the previous conclusions based on comparisons of spectral interactions of the ligands [27]. This interaction leads to apparently enhanced binding of $(CH_3)_2CH\text{-}O\text{-}PhNO_2$ in the presence of $Ph(NC)_2$ (and vice-versa) [27] but results in inhibition of catalytic activity (Fig. 4), even when the substrate is $(CH_3)_2CH\text{-}O\text{-}PhNO_2$ (Fig. 4a). We proposed that co-occupancy of the P450 1A2 active site is a common feature of numerous small substrates (and other ligands) but the nature of cooperative behavior is highly ligand dependent [27,28]. Apparently loading the active site with two molecules of $(CH_3)_2CH\text{-}O\text{-}PhNO_2$ moves the substrate into a less favorable conformation for oxidation, explaining the attenuated catalytic efficiency at higher substrate concentrations [27]. The interaction of P450 1A2 with $Ph(NC)_2$ increases the spectrally detectable binding of $(CH_3)_2CH\text{-}O\text{-}PhNO_2$ to P450 1A2 [27] but apparently does so in a way that attenuates catalytic activity (Fig. 4). In our earlier work [27] with this isocyanide and substrate, the titration results provided evidence that each compound could enhance the binding of the other. We postulate that one factor in binding of $Ph(NC)_2$ is the interaction of the phenyl ring somewhere in the active site. One option for binding is that shown in Fig. 6b, in which the substrate ($(CH_3)_2CH\text{-}O\text{-}PhNO_2$) is bound near the iron atom,

in juxtaposition for oxidation at the CH position. This configuration may be possible but apparently a mode such as that shown in Fig. 6c is more dominant, as reflected in the inhibition (Fig. 4). A major point of the present work is that one can get cooperativity in binding of ligands but that this does not necessarily translate to catalytic activity, e.g. see [56].

In summary, we have been able to extend earlier observations on the heterotropic cooperativity of rabbit P450 1A2 [27]. The modeling is clearly consistent with the previously presented proposal that one molecule each of $Ph(NC)_2$ and $(CH_3)_2CH\text{-}O\text{-}PhNO_2$ can co-occupy the active site. However, the heterotropic cooperativity yields enhancement of substrate binding but not an increase in catalytic activity. Apparently the juxtoposition of the 1-alkoxy-4-nitrobenzene imposed by the $Ph(NC)_2$ ligand is unfavorable for catalysis in this case, although the nature of such an interaction was not revealed in the modeling.

Acknowledgments

This work was supported in part by U.S. Public Health Service (USPHS) Grants R37 CA090426 (F.P.G.), T32 ES007028 (C.D.S., F.P.G.), F32 CA119776 (R.L.E.), and P30 ES000267 (F.P.G.). We thank M. V. Martin for preparing some of the enzymes, W. M. Backes (Louisiana State University, New Orleans) for some of the rabbit liver samples used in enzyme purification, R. N. Armstrong for use of the stopped-flow spectrophotometer for CD studies, L. Mizoue for assistance with the JASCO CD spectrometer, and K. Trisler for assistance in preparation of the manuscript.

References

1. Palmer G, Reedijk J. J. Biol. Chem. 1992; 267:665–677. [PubMed: 1309757]
2. Ortiz de Montellano, PR. Cytochrome P450: Structure, Mechanism, and Biochemistry. 3rd ed.. New York: Kluwer Academic/Plenum Publishers; 2005.
3. Williams JA, Hyland R, Jones BC, Smith DA, Hurst S, Goosen TC, Peterkin V, Koup JR, Ball SE. Drug Metab. Dispos. 2004; 32:1201–1208. [PubMed: 15304429]
4. Wienkers LC, Heath TG. Nat. Rev. Drug Discov. 2005; 4:825–833. [PubMed: 16224454]
5. Segel, IH. Enzyme Kinetics. New York: Wiley; 1975.
6. Kuby, SA. A Study of Enzymes, Vol. I, Enzyme Catalysis, Kinetics, and Substrate Binding. Boca Raton, FL: CRC Press; 1991.
7. Cinti DL. Pharmacol. Ther. 1978; 2:727–749.
8. Kapitulnik J, Poppers PJ, Buening MK, Fortner JG, Conney AH. Clin. Pharmacol.Ther. 1977; 22:475–485. [PubMed: 902460]
9. Lasker JM, Huang M-T, Conney AH. Science. 1982; 216:1419–1421. [PubMed: 7089530]
10. Guengerich, FP.; Kim, B-R.; Gillam, EMJ.; Shimada, T. Proceedings, 8th Int. Conf. on Cytochrome P450: Biochemistry, Biophysics, and Molecular Biology. In: Lechner, MC., editor. John Libbey Eurotext; Paris. 1994. p. 97-101.
11. Shou M, Grogan J, Mancewicz JA, Krausz KW, Gonzalez FJ, Gelboin HV, Korzekwa KR. Biochemistry. 1994; 33:6450–6455. [PubMed: 8204577]
12. Guengerich, FP. Cytochrome P450: Structure, Mechanism, and Biochemistry. 3rd ed.. Ortiz de Montellano, PR., editor. New York: Kluwer Academic/Plenum Publishers; 2005. p. 377-530.
13. Atkins WM. Expert Opin. Drug Metab. Toxicol. 2006; 2:573–579. [PubMed: 16859405]
14. Tracy TS. Drugs Res. Devlop. 2006; 7:349–363.
15. Johnson EF, Schwab GE, Dieter HH. J. Biol. Chem. 1983; 258:2785–2788. [PubMed: 6826540]
16. Schwab GE, Raucy JL, Johnson EF. Mol. Pharmacol. 1988; 33:493–499. [PubMed: 3367901]
17. Harlow GR, Halpert JR. Proc. Natl. Acad. Sci. USA. 1998; 95:6636–6641. [PubMed: 9618464]
18. Hosea NA, Miller GP, Guengerich FP. Biochemistry. 2000; 39:5929–5939. [PubMed: 10821664]

19. Koley AP, Buters JTM, Robinson RC, Markowitz A, Friedman FK. J. Biol. Chem. 1997; 272:3149–3152. [PubMed: 9013547]
20. Fernando H, Davydov DR, Chin CC, Halpert JR. Arch. Biochem. Biophys. 2007; 460:129–140. [PubMed: 17274942]
21. Jushchyshyn MI, Hutzler JM, Schrag ML, Wienkers LC. Arch. Biochem. Biophys. 2005; 438:21–28. [PubMed: 15910734]
22. Yano JK, Wester MR, Schoch GA, Griffin KJ, Stout CD, Johnson EF. J. Biol. Chem. 2004:38091–38094. [PubMed: 15258162]
23. Williams PA, Cosme J, Vinkovic DM, Ward A, Angove HC, Day PJ, Vonrhein C, Tickle IJ, Jhoti H. Science. 2004; 305:683–686. [PubMed: 15256616]
24. Schoch GA, Yano JK, Wester MR, Griffin KJ, Stout CD, Johnson EF. J. Biol. Chem. 2004; 279:9497–9503. [PubMed: 14676196]
25. Wester MR, Yano JK, Schoch GA, Yang C, Griffin KJ, Stout CD, Johnson EF. J. Biol. Chem. 2004; 279:35630–35637. [PubMed: 15181000]
26. Sansen S, Yano JK, Reynald RL, Schoch G, Griffin K, Stout CD, Johnson EF. J. Biol. Chem. 2007; 282:14348–14355. [PubMed: 17311915]
27. Miller GP, Guengerich FP. Biochemistry. 2001; 40:7262–7272. [PubMed: 11401574]
28. Sohl CD, Isin EM, Eoff RL, Marsch GA, Stec DF, Guengerich FP. J. Biol. Chem. 2008; 283 in press (PMID: 18187423).
29. Warburg O, Negelein E, Christian W. Biochem. Z. 1929; 214:26–63.
30. Imai Y, Sato R. J. Biochem. (Tokyo). 1968; 63:380–389. [PubMed: 4386148]
31. Ichikawa Y, Yamano T. Biochim. Biophys. Acta. 1968; 153:753–765. [PubMed: 4385526]
32. Imai, Y.; Horie, S.; Yamano, T.; Iizuka, T. Cytochrome P-450. Sato, R.; Omura, T., editors. New York: Academic Press; 1978. p. 37-135.
33. Lee D-S, Park S-Y, Yamane K, Obayashi E, Hori H, Shiro Y. Biochemistry. 2001; 40:2669–2677. [PubMed: 11258878]
34. Sandhu P, Guo Z, Baba T, Martin MV, Tukey RH, Guengerich FP. Arch. Biochem. Biophys. 1994; 309:168–177. [PubMed: 8117105]
35. Alterman MA, Dowgii AI. Biomed. Chromatog. 1990; 4:221–222. [PubMed: 2279149]
36. Hanna IH, Teiber JF, Kokones KL, Hollenberg PF. Arch. Biochem. Biophys. 1998; 350:324–332. [PubMed: 9473308]
37. Guengerich, FP.; Bartleson, CJ. Principles and Methods of Toxicology. 5th ed.. Hayes, AW., editor. Boca Raton, FL: CRC Press; 2007. p. 1981-2048.
38. Ueng Y-F, Kuwabara T, Chun Y-J, Guengerich FP. Biochemistry. 1997; 36:370–381. [PubMed: 9003190]
39. Imai Y, Ito A, Sato T. J. Biochem. (Tokyo). 1966; 60:417–428. [PubMed: 4291137]
40. Shumyantseva VV, Bulko TV, Bachmann TT, Bilitewski U, Schmid RD, Archakov AI. Arch. Biochem. Biophys. 2000; 377:43–48. [PubMed: 10775439]
41. Chetiyanukornkul T, Toriba A, Kizu R, Makino T, Nakazawa H, Hayakaw K, Chromatog J. 2002; A 961:107–112.
42. Burleigh BD Jr, Foust GP, Williams CH Jr. Anal. Biochem. 1969; 27:536–544. [PubMed: 5767207]
43. Foust GP, Burleigh BD Jr, Mayhew SG, Williams CH Jr, Massey V. Anal. Biochem. 1969; 27:530–535. [PubMed: 5767206]
44. Guengerich FP, Krauser JA, Johnson WW. Biochemistry. 2004; 43:10775–10788. [PubMed: 15311939]
45. Schwede T, Kopp J, Guex N, Peitsch MC. Nucl. Acids Res. 2003; 31:3381–3385. [PubMed: 12824332]
46. Schuttelkopf AW, van Aalten DM. Acta Crystallogr. D Biol. Crystallogr. 2004; 60:1355–1363. [PubMed: 15272157]

47. Brunger AT, Adams PD, Clore GM, DeLano WL, Gros P, Grosse-Kunstleve RW, Jiang JS, Kuszewski J, Nilges M, Pannu NS, Read RJ, Rice LM, Simonson T, Warren GL. Acta Crystallogr. D Biol. Crystallogr. 1998; 54:905–921. [PubMed: 9757107]
48. Rice LM, Brunger AT. Proteins. 1994; 19:277–290. [PubMed: 7984624]
49. Greenfield N, Fasman GD. Biochemistry. 1969; 8:4108–4116. [PubMed: 5346390]
50. Yun C-H, Miller GP, Guengerich FP. Biochemistry. 2001; 40:4521–4530. [PubMed: 11284709]
51. Gotoh O. J. Biol. Chem. 1992; 267:83–90. [PubMed: 1730627]
52. Quattrochi LC, Pendurthi UR, Okino ST, Potenza C, Tukey RH. Proc. Natl. Acad. Sci. USA. 1986; 83:6731–6735. [PubMed: 3462722]
53. O'Haver TC, Green GL. Anal. Chem. 1976; 48:312–318.
54. Guengerich FP. Biochemistry. 1983; 22:2811–2820. [PubMed: 6307349]
55. Fersht, A. Structure and Mechanism in Protein Science. New York: Freeman; 1999. p. 158-161.
56. Lampe JN, Fernandez C, Nath A, Atkins WM. Biochemistry. 2008; 47:509–516. [PubMed: 18092806]

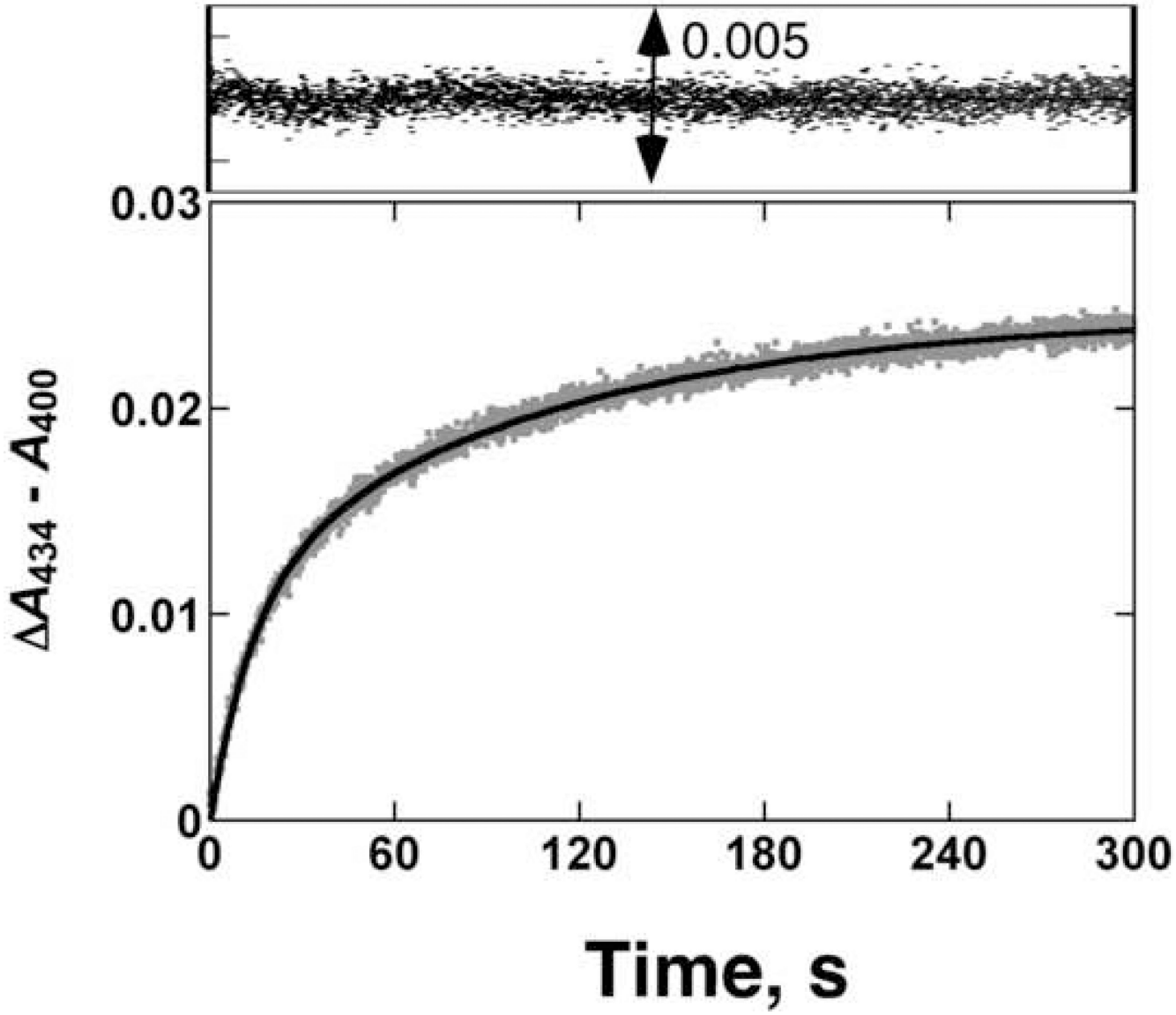

Fig. 1. Pre-steady-state kinetics of $Ph(NC)_2$ binding to ferric P450 1A2

The kinetic trace (ΔA_{434}–A_{400}) obtained for $Ph(NC)_2$ (100 μM) binding to P450 1A2 (1 μM) was fit to a bi-exponential plot with rates of 0.07 and 0.01 s^{-1}.

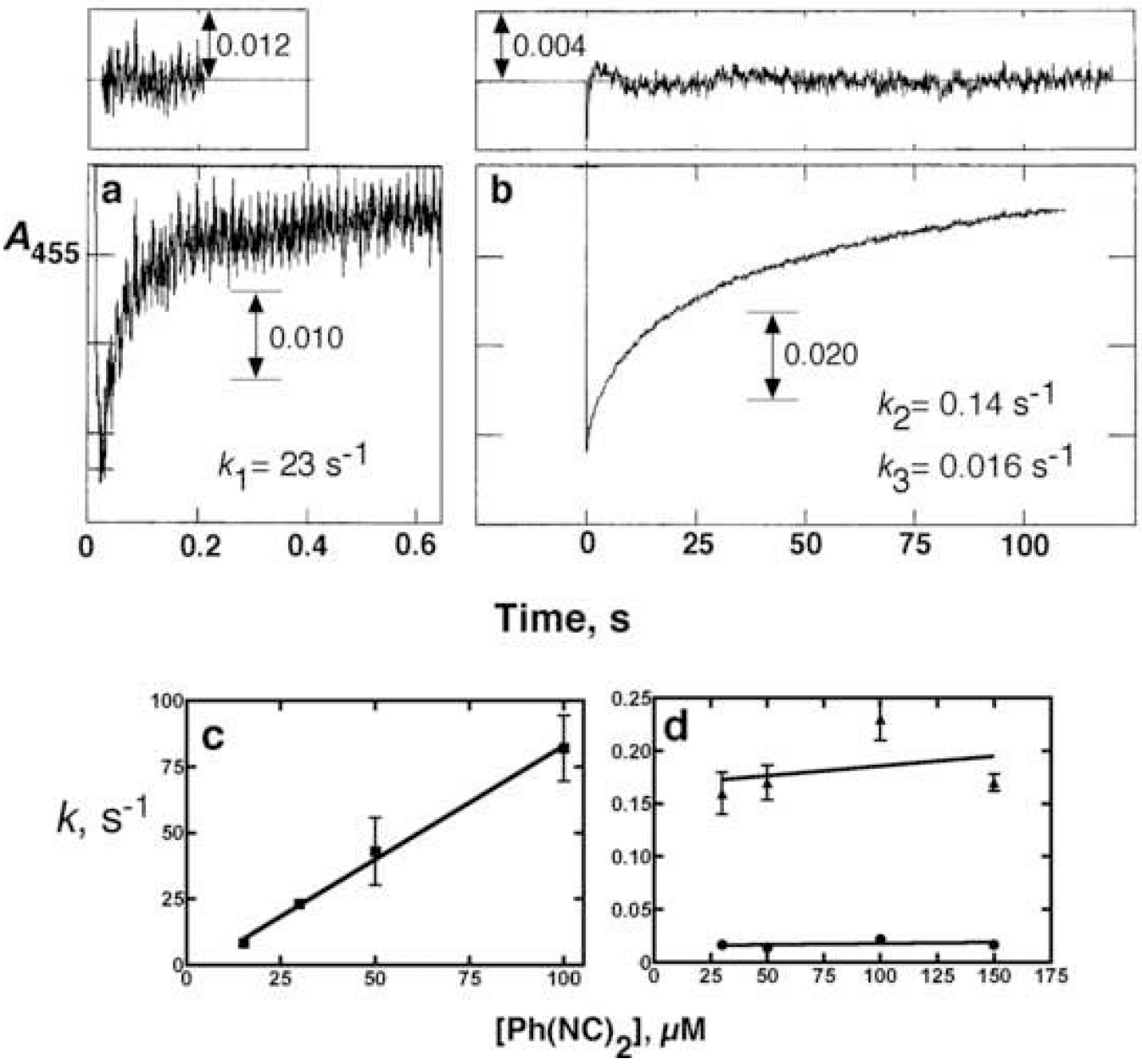

Fig. 2. Pre-steady-state kinetics of ligand binding to ferrous P450 1A2

P450 1A2 (1.0 μM final concentration following mixing) was reduced anaerobically in the presence of 0.25 μM NADPH-P450 reductase (and 75 μM L-α-dilauroyl-*sn*-glycero-3-phosphocholine and an NADPH-generating system [36]. (a) First portion of reaction with 30 μM (final concentration) of anaerobic $Ph(NC)_2$. The initial part of the trace was fit to a single exponential of $k_1 = 23 \pm 0.2$ s^{-1}. (b) Latter phases of the reaction were fit to a biexponential plot with $k_2 = 0.14 \pm 0.01$ s^{-1} and $k_3 = 0.016 \pm 0.003$ s^{-1}. (c) Rates of k_1 were determined at varying concentration of $Ph(NC)_2$ and fit to a plot, with an intercept near 0 and a calculated second-order rate of 1.4 (± 0.1) × 10^6 M^{-1} s^{-1}. (d) Values of k_2 and k_3 as a function of $Ph(NC)_2$ concentration.

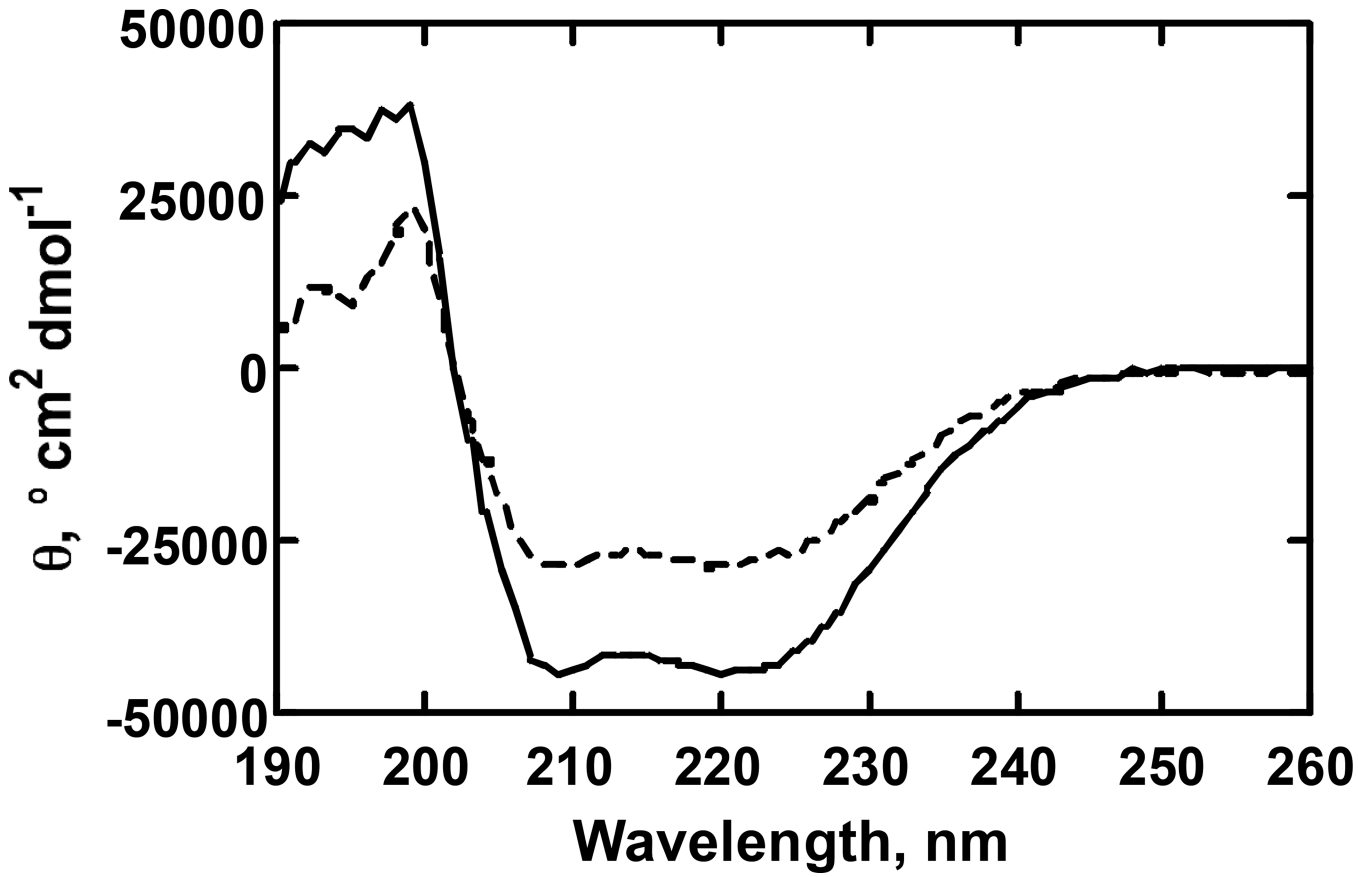

Fig. 3. CD spectra of $Ph(NC)_2$ binding to rabbit P450 1A2

The solid line (—) is a scan with 0.41 μM P450 1A2 alone and the dotted line (----) is the scan following the addition of $Ph(NC)_2$ (40 μM), followed by a 15 min incubation. The cuvette pathlength was 1 mm and A_{220} was < 0.2 in both cases.

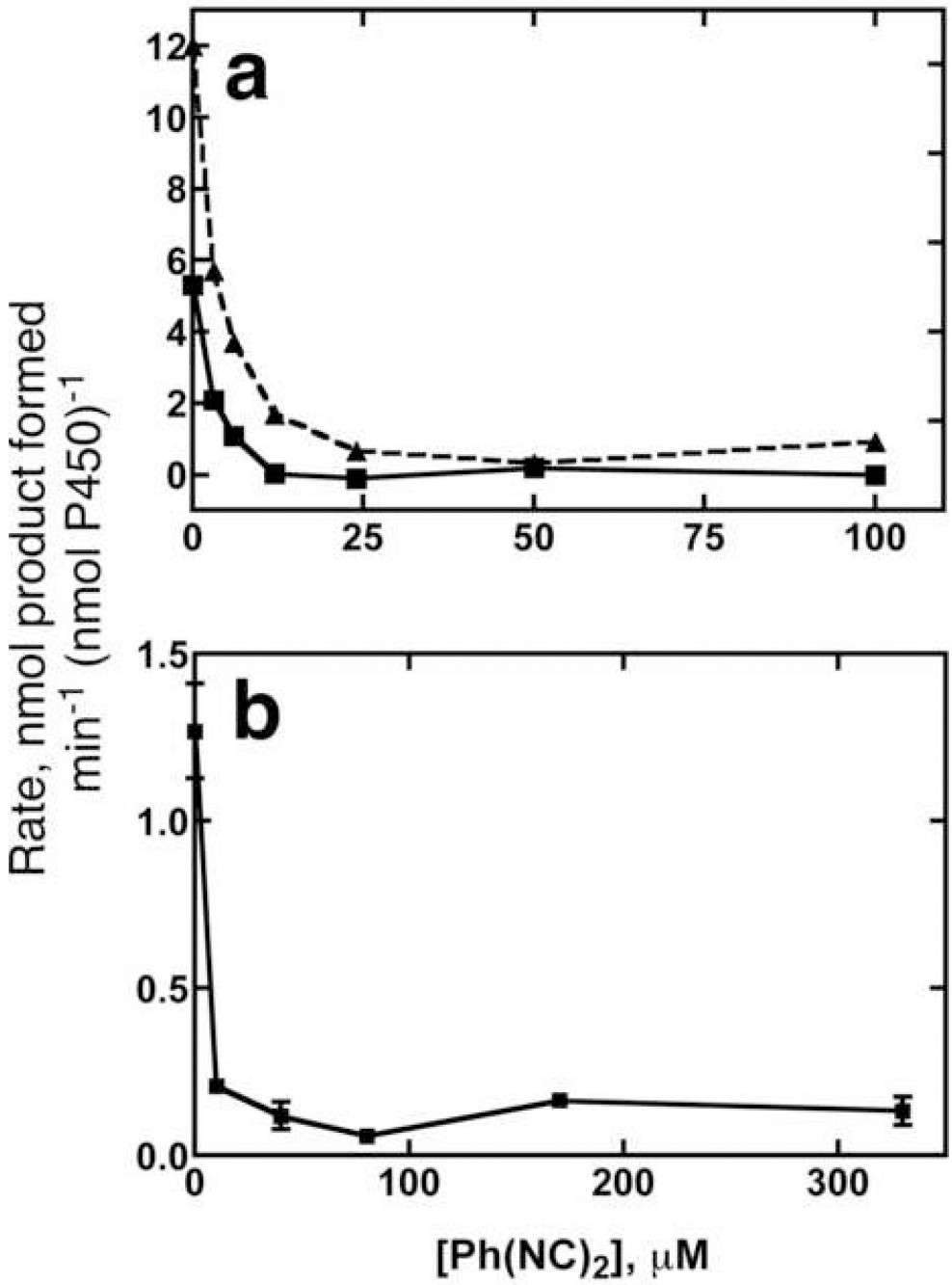

Fig. 4. Inhibition of P450 1A2 catalytic activity

(a) $(CH_3)_2CH$-O-$PhNO_2$ *O*-dealkylation, as measured by absorbance at 400 nm. The data were fit to a straight line to determine the amount of 4-nitrophenol formed per min. The dotted line (----) shows the rate of *O*-dealkylation of 700 μM $(CH_3)_2CH$-O-P-hNO_2 and the solid line (—) line shows the rates measured with 50 μM $(CH_3)_2CH$-O-$PhNO_2$. (b) Aniline 4-hydroxylation. Formation of *p*-aminophenol (substrate concentration of 8 mM aniline) was monitored by measuring absorbance at 630 nm after derivatization.

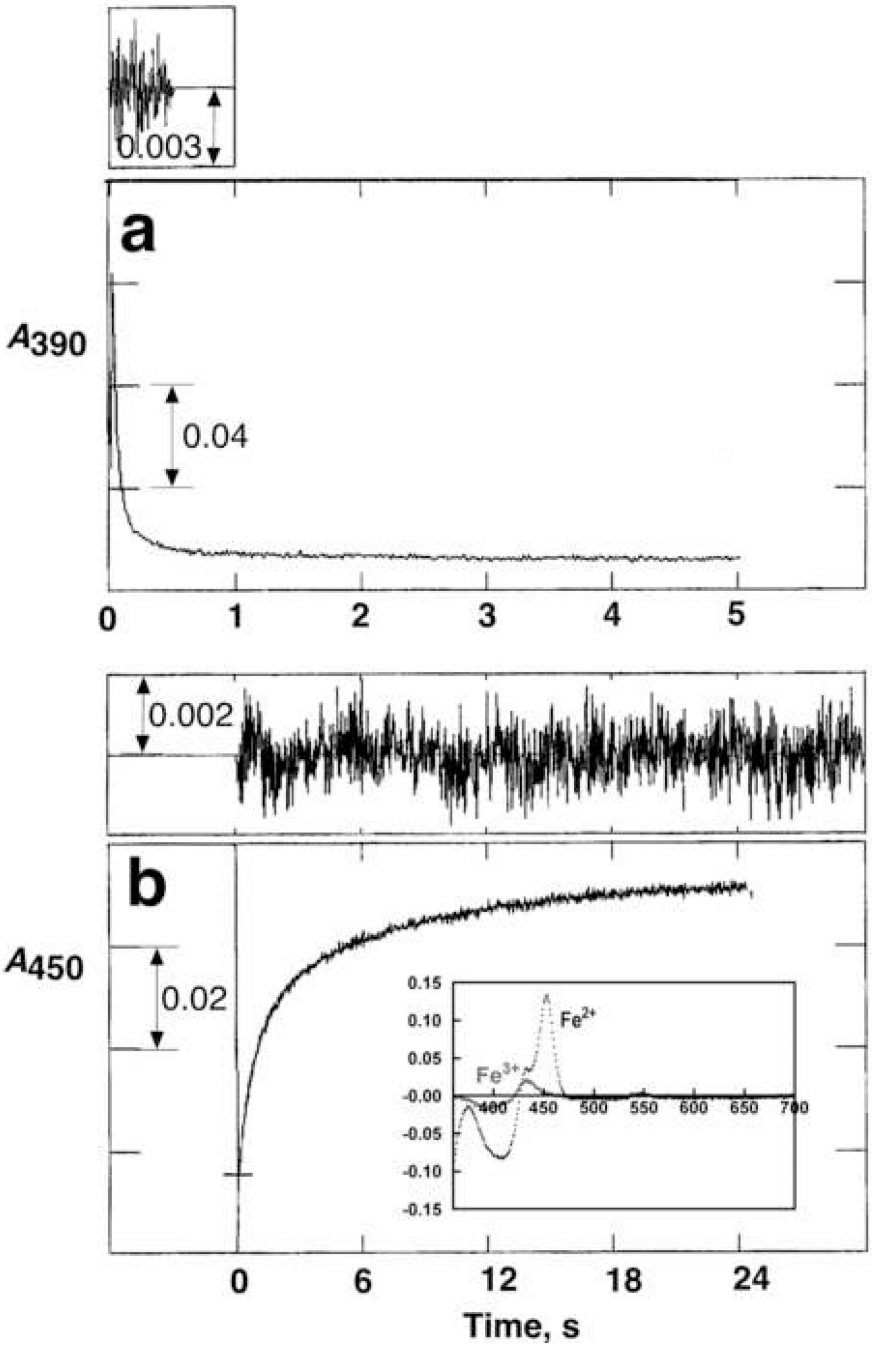

Fig. 5. Effect of $Ph(NC)_2$ on rate of enzymatic reduction of P450 1A2

All experiments included 2.0 μM P450 1A2, 4.0 μM NADPH-P450 reductase, and 75 μM L-α-dilauroyl*sn*-glycero-3-phosphocholine, with the reaction initiated by the addition of 100 μM NADPH (23 °C, anaerobic conditions, argon atmosphere). (a) Reduction in absence of ligands, measured at 390 nm. The first part of the trace was fit to a single exponential with a rate of 25 (± 1) s^{-1}. (b) Reduction in the presence of 100 μM $Ph(NC)_2$, measured at 455 nm. The data were fit to a bi-exponential plot with k_1 = 1.3 ± 0.02 s^{-1} and k_2 = 0.14 ± 0.002 s^{-1}. Residuals traces for the fits are shown in both parts a and b. The inset in Part b shows the

difference spectra generated by the addition of 100 μM $Ph(NC)_2$ to ferric (peak near 430 nm, trough at 395 nm) and ferrous (peak at 455 nm, trough at 405 nm) P450 1A2 (2.0 μM).

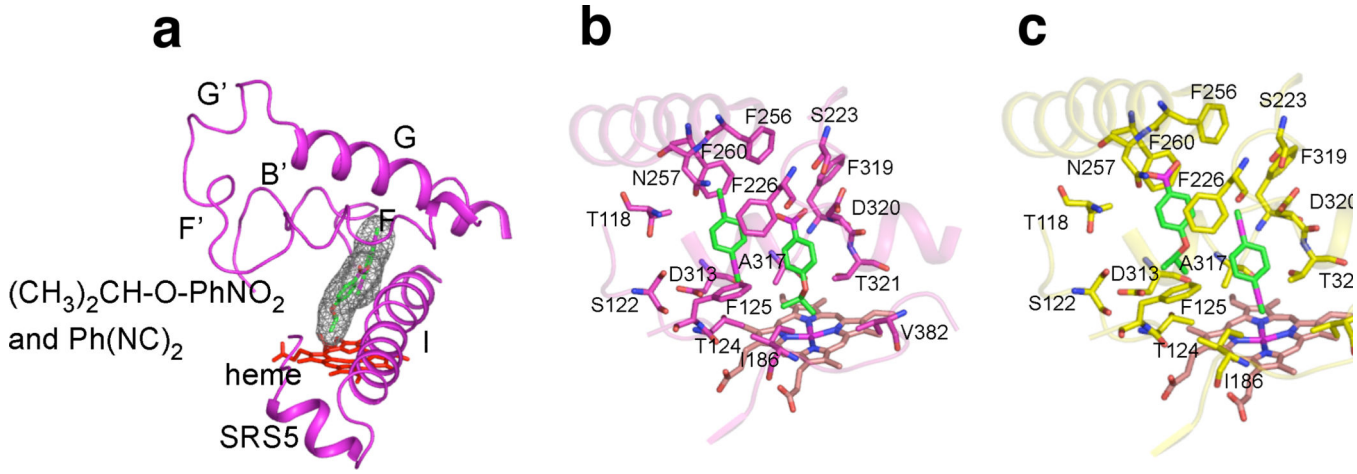

Fig. 6. Docking of ligands into homology model of rabbit P450 1A2

(a) Rabbit P450 1A2 homology model (magenta ribbon) with heme group (red sticks) and $(CH_3)_2CH$-O-$PhNO_2$ plus $Ph(NC)_2$ (sticks with space-filling mesh). SRS5: Substrate recognition sequence 5 [51]. (b) Active-site of rabbit P450 1A2 homology model (magenta ribbon) with heme group (sticks) and $(CH_3)_2CH$-O-$PhNO_2$ plus $Ph(NC)_2$ (sticks), with $(CH_3)_2CH$-O-$PhNO_2$ modeled close to heme Fe in the most productive mode and sidechains highlighted. (c) Active-site of rabbit P450 1A2 homology model (yellow ribbon) with heme group (sticks) and $Ph(NC)_2$ plus $(CH_3)_2CH$-O-$PhNO_2$ (sticks), with $Ph(NC)_2$ liganded to heme Fe and side chains highlighted.